

# ALDEN: REINFORCEMENT LEARNING FOR ACTIVE NAVIGATION AND EVIDENCE GATHERING IN LONG DOCUMENTS

006 **Anonymous authors**

007 Paper under double-blind review

## ABSTRACT

013 Vision–language models (VLMs) excel at interpreting text-rich images but strug-  
 014 gle with long, visually complex documents that demand analysis and integration  
 015 of information spread across multiple pages. Existing approaches typically rely  
 016 on fixed reasoning templates or rigid pipelines, which force VLMs into a pas-  
 017 sive role and hinder both efficiency and generalization. We present Active Long-  
 018 DocumEnt Navigation (ALDEN), a multi-turn reinforcement learning framework  
 019 that fine-tunes VLMs as interactive agents capable of actively navigating long,  
 020 visually rich documents. ALDEN introduces a novel `fetch` action that directly  
 021 accesses the page by index, complementing the classic `search` action and bet-  
 022 ter exploiting document structure. For dense process supervision and efficient  
 023 training, we propose a rule-based cross-level reward that provides both turn-  
 024 and token-level signals. To address the empirically observed training instabil-  
 025 ity caused by numerous visual tokens from long documents, we further propose  
 026 a visual-semantic anchoring mechanism that applies a dual-path KL-divergence  
 027 constraint to stabilize visual and textual representations separately during train-  
 028 ing. Trained on a corpus constructed from three open-source datasets, ALDEN  
 029 achieves state-of-the-art performance on five long-document benchmarks. Over-  
 030 all, ALDEN marks a step beyond passive document reading toward agents that  
 031 autonomously navigate and reason across long, visually rich documents, offering  
 032 a robust path to more accurate and efficient long-document understanding. All  
 033 code and datasets will be released on to support future research.

## 1 INTRODUCTION

036 Visually rich documents (VRDs) serve as primary vehicles for storing and communicating structured  
 037 knowledge in real-world applications. Unlike plain text, these documents combine different modal-  
 038 ities, including text, tables, and figures, embedded in human-friendly layouts that encode semantic  
 039 relationships. Effectively understanding such documents requires not only extracting textual content  
 040 but also reasoning over their visual and structural organization. This has given rise to the task of  
 041 visually rich document understanding (VRDU) (Wang et al., 2023; Ding et al., 2022) which aims  
 042 to develop systems to automatically analyze VRDs and answer user queries, underpinning various  
 043 practical applications (Liang et al., 2024; Rombach & Fettke, 2024)

044 Despite recent progress of vision–language models (VLMs) on single-page or short documents (Xie  
 045 et al., 2024; Lv et al., 2023; Hu et al., 2024), real-world long documents spanning dozens or even  
 046 hundreds of pages remain highly challenging. Feeding entire documents into a model’s context is  
 047 computationally expensive and introduces substantial noise, making it difficult for VLMs to focus  
 048 on relevant pages (Cho et al., 2024). A more scalable alternative is to have the VLM reason only  
 049 over semantically relevant pages retrieved by a multimodal retriever (Faysse et al., 2025), following  
 050 the retrieval-augmented generation (RAG) paradigm (Cho et al., 2024; Chen et al., 2025a). Recent  
 051 work has extended this idea by building prompting-based pipeline in which VLMs passively perform  
 052 predefined subtasks such as query reformulation or retrieval analysis within fixed workflows (Han  
 053 et al., 2025; Wang et al., 2025b). While effective, these systems rely on static reasoning patterns  
 This motivates shifting the research focus to the **Agentic VRDU** (A-VRDU) task, which requires

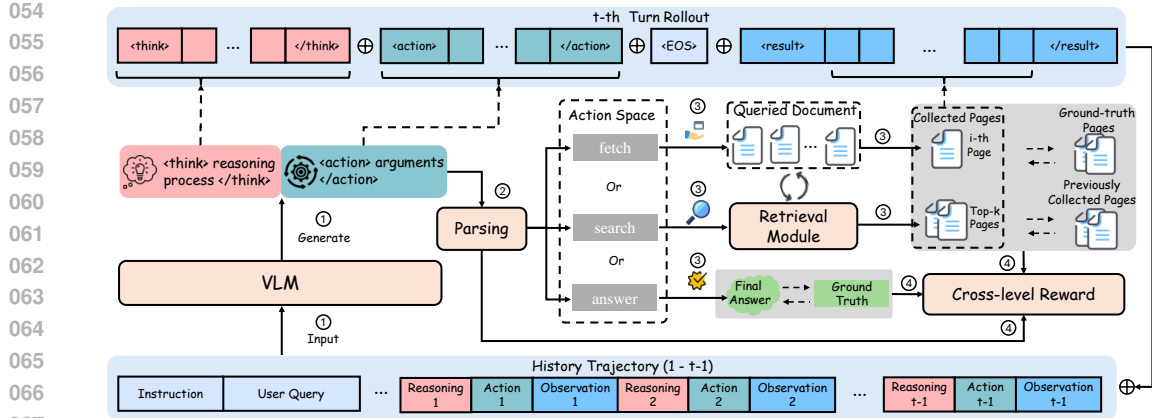


Figure 1: Overview of the rollout process. At each turn: (1) the VLM generates a response conditioned on the dialogue history; (2) the response is parsed into an action (search, fetch, or answer); (3) the action is executed, where search or fetch collect document pages and answer terminates the process; and (4) the cross-level reward function assigns rewards based on execution outcomes and parsing results.

the model to act as an agent that can actively navigate and reason over long documents to deliver accurate and adaptive question answering beyond fixed RAG pipelines.

Recent studies (Chen et al., 2025b; Jin et al., 2025; Song et al., 2025) show that modeling search as an action and optimizing the workflow with outcome-based RL yields more generalizable agents that can actively gather information from external databases, offering a promising direction for the open problem of A-VRDU. However, extending this framework to fine-tune VLMs for A-VRDU poses unique challenges. User queries often reference specific documents, page numbers, or require reasoning across consecutive pages, where generic semantic retrieval is inefficient. Moreover, document-level information gathering typically demands multi-turn interaction with retrieval models, where sparse and delayed outcome-based rewards fail to reinforce helpful intermediate steps or discourage redundant actions. A further challenge arises from the high-dimensional visual inputs. We empirically observe that fully masking the visual tokens when computing the policy gradient, as in existing approaches, leads to unstable training dynamics and can even cause collapse.

These limitations motivate our framework, **Active Long-DocumEnt Navigation** (ALDEN), a multi-turn RL framework that trains VLMs as interactive agents for navigation in long, visually-rich documents. The overall reasoning-action rollout of ALDEN is illustrated in Fig. 1. ALDEN expands the action space by introducing the `fetch` action, which enables direct page-index access to complement search-based retrieval and efficiently handle diverse queries. We incorporate a *cross-level reward function* as opposed to the sparse outcome-based reward typically used, which integrates rule-based turn-level supervision with a token-level repetition penalty to provide fine-grained process supervision, encouraging informative evidence collection while discouraging repeated query formulations. Finally, ALDEN incorporates a *visual semantic anchoring* mechanism, which constrains the hidden states of generated and visual tokens separately during training to preserve the grounding of visual-token representations and improve overall training robustness.

We build a training corpus from DUDE (Van Landeghem et al., 2023), MPDocVQA (Tito et al., 2023b), and SlideVQA (Tanaka et al., 2023b) to train an A-VRDU agent with ALDEN and evaluate it on five benchmarks. Experimental results show that ALDEN achieves state-of-the-art performance over strong baselines and demonstrates the effectiveness of its key components. Overall, the A-VRDU task establishes a new paradigm for processing practical, lengthy VRDs, shifting from passive document reading to autonomous navigation and reasoning. ALDEN’s strong results validate this paradigm and provide guidance for building efficient, robust A-VRDU agents from VLMs.

Overall, our main contribution can be summarized as follows:

- We propose the agentic visually-rich document understanding (A-VRDU) task that aims to develop agents that can actively navigate and reason over long visually-rich documents.
- To perform the A-VRDU task, we introduce **ALDEN**, a multi-turn RL framework with three key components: an expanded action space featuring a novel `fetch` action, a cross-level reward

108 function, and a visual semantic anchoring mechanism, which together enable efficient and robust  
 109 training.

110 • We construct a training corpus for training the A-VRDU agent and conduct extensive experiments  
 111 on five commonly used VRDU benchmarks, showing that ALDEN significantly outperforms the  
 112 strongest baseline, improving the answer accuracy by 9.14% on average.

113

## 114 2 RELATED WORK

### 117 2.1 VISUALLY-RICH DOCUMENTS UNDERSTANDING

119 Recent VLMs that process document images directly without OCR (Hu et al., 2024; Xie et al., 2024;  
 120 Feng et al., 2024; Liu et al., 2024b) have shown strong performance on single-page or short-  
 121 document benchmarks (Mathew et al., 2021; Masry et al., 2022; Mathew et al., 2022). In contrast,  
 122 real-world documents often span dozens or hundreds of pages, requiring reasoning across dispersed  
 123 text, tables, and figures (Deng et al., 2024; Ma et al., 2024b). Extending context length to encode  
 124 entire documents (Tito et al., 2023b; Blau et al., 2024) is computationally prohibitive and introduces  
 125 noise, while semantic retrieval provides a more scalable way to focus on relevant pages (Chen et al.,  
 126 2025b; Jin et al., 2025; Song et al., 2025). However, existing retrieval-based methods largely rely on  
 127 prompting-based workflows (Han et al., 2025; Wang et al., 2025b), which are static and brittle. In  
 128 contrast, we study A-VRDU task, and propose to fine-tune VLMs with RL, enabling them to serve  
 129 as VRDU agents capable of active, multi-step retrieval and reasoning.

130

### 131 2.2 RL TRAINING FOR LLMs/VLMs

133 RL was introduced to LLM fine-tuning by Ouyang et al. (2022); Ziegler et al. (2019) through  
 134 reinforcement learning from human feedback (RLHF), where a learned reward model guides the  
 135 RL-based tuning of the policy LLM typically via the Proximal Policy Optimization (PPO) algo-  
 136 rithm (Schulman et al., 2017). Recently, RL with verifiable outcome-based rewards (RLVR) (Shao  
 137 et al., 2024) further demonstrates impressive effect in inducing sophisticated reasoning ability in  
 138 LLMs. Building on this progress, several recent studies integrate RL with retrieval-augmented gen-  
 139 eration (RAG), fine-tuning LLMs as agents that actively gather evidence through retrieval and reason  
 140 over it (Jin et al., 2025; Song et al., 2025). However, extending these methods to the A-VRDU task  
 141 remains largely unexplored. Unlike open-domain retrieval, VRDU requires exploiting explicit doc-  
 142 ument structure (e.g., page indices), denser supervision to guide multi-turn navigation, and stability  
 143 against the large number of unconstrained visual tokens introduced by high-resolution document  
 144 pages, motivating new RL frameworks tailored for this task.

145

## 146 3 PRELIMINARIES

147

### 148 3.1 PROBLEM FORMULATION

149

150 In the A-VRDU task, a user query  $q_u$  is paired with a document  $\mathcal{D} = (p_1, p_2, \dots, p_{|\mathcal{D}|})$  that can  
 151 only be accessed through specific ways, where  $p_i$  denotes the  $i$ -th page and  $|\mathcal{D}|$  the total number  
 152 of pages. The goal is to build an agent that can actively analyzes available information, decides  
 153 whether and how to collect additional pages from the document, and ultimately generates a final  
 154 answer  $y'$  based on the collected evidence. This sequential decision-making process can be naturally  
 155 formulated as a Markov Decision Process (MDP) (Bellman, 1957). Formally, at each turn  $t$ , the  
 156 agent generates an action  $a_t$  from the action space  $\mathcal{A}$ . Upon executing the action, the document  
 157 returns a visual observation  $o_t \in \mathcal{O}$  (i.e., a page image) and a scalar reward  $r_t \in \mathbb{R}$ , which reflects  
 158 the action's utility in acquiring useful evidence or answering the query. The state  $s_t$  is defined as the  
 159 interaction history up to turn  $t$ , given by  $s_t = [x, a_1, o_1, \dots, a_{t-1}, o_{t-1}]$ , where  $x$  denotes the initial  
 160 prompt constructed from the query and task instructions. The agent's objective is to maximize the  
 161 expected cumulative reward  $\sum_{t=1}^T \gamma^t r(s_t, a_t)$ , where  $T$  is the maximum number of interaction turns  
 per episode,  $\gamma$  denotes the discount factor.

162 3.2 PROXIMAL POLICY OPTIMIZATION FOR FINE-TUNING LLMs  
163

164 PPO algorithm is an actor-critic RL algorithm that has been widely used in RLHF to fine-tune  
165 language models toward task-specific preferences. In the classical RLHF setup, the problem is  
166 typically modeled as a contextual bandit, where each episode involves a single interaction step.  
167 Formally, given an input prompt  $x$ , the LLM auto-regressively generates a variable-length token  
168 sequence  $(a_1^1, \dots, a_1^L) \in \mathcal{V}^L$  as a single action  $a_1$  where  $\mathcal{V}$  denotes the vocabulary and  $L$  is the  
169 sequence length. A scalar reward  $r_1$  is assigned to the action by a learned reward model. Since  
170 LLMs operate token-by-token, PPO is actually applied at the token level by treating each token  
171  $a_1^i \in \mathcal{V}$  as an action, with state  $s_1^i = (x, a_1^1, \dots, a_1^{i-1})$  defined as the prompt concatenated with the  
172 partial response. To propagate the turn-level reward  $r_1$  to individual tokens, a token-level reward  
173 signal is assigned as

$$174 \quad r_1^i = \begin{cases} r_1 - \beta \cdot \text{KL}[\pi_\theta(a_1^i | s_1^i) || \pi_{\text{ref}}(a_1^i | s_1^i)], & \text{if } i = L \\ -\beta \cdot \text{KL}[\pi_\theta(a_1^i | s_1^i) || \pi_{\text{ref}}(a_1^i | s_1^i)], & \text{otherwise} \end{cases} \quad (1)$$

175 where  $\pi_{\text{ref}}$  is the reference model (e.g., a frozen copy of the pre-trained LLM), the  $\text{KL}(\cdot)$  term  
176 acts as a penalty to prevent the policy from drifting too far from the reference model,  $\beta$  is the  
177 hyperparameter to control the weight of the KL divergence penalty. In addition to the policy  $\pi_\theta$ , a  
178 value function  $V_\phi(s_1^i)$  is trained to predict the expected return at each token position. Generalized  
179 Advantage Estimation (GAE) (Schulman et al., 2015) is generally used to calculate the advantage  
180 of each token-level action:

$$181 \quad A_1^i = \sum_{k=i}^L (\gamma_{\text{token}} \lambda_{\text{token}})^{k-i} \delta_k, \quad \delta_k = r_1^k + \gamma_{\text{token}} V_\phi(s_1^{k+1}) - V_\phi(s_1^k) \quad (2)$$

182 where  $\lambda \in [0, 1]$  is a hyperparameter to balance the estimation bias and variance. The value function  
183 is then optimized by minimizing the mean squared error between predicted values and GAE-  
184 estimated target values  $\hat{V}_1^i = A_1^i + V_\phi(s_1^i)$ . The LLM is finally optimized by maximizing the  
185 following surrogate objective:

$$186 \quad \mathcal{L}_{\text{policy}} = \mathbb{E}_x \left[ \sum_{i=1}^L \left[ \min \left[ \frac{\pi_\theta(a_1^i | s_1^i)}{\pi_{\text{old}}(a_1^i | s_1^i)} A_1^i, \text{clip} \left( \frac{\pi_\theta(a_1^i | s_1^i)}{\pi_{\text{old}}(a_1^i | s_1^i)}, 1 - \epsilon, 1 + \epsilon \right) A_1^i \right] \right] \right] \quad (3)$$

187 where  $\pi_\theta$  and  $\pi_{\text{old}}$  are the current and old policy models,  $\epsilon$  is a clipping-related hyper-parameter introduced  
188 in PPO for stabilizing training. The single-turn PPO framework propagates only immediate  
189 rewards to tokens, neglecting each action's contribution to final task completion and fine-grained token  
190 supervision. We next describe how we adapt it for long-horizon, multi-turn interaction in the  
191 A-VRDU task.

## 192 4 METHODOLOGY

193 We propose **Active Long-DocumEnt Navigation (ALDEN)**, a reinforcement learning framework for  
194 training VLMs as interactive agents that can actively navigate and reason over long, visually rich  
195 documents by operating in a multi-turn reasoning-action loop, incrementally collecting evidence  
196 pages until a question can be confidently answered. To this end, ALDEN introduces three key  
197 components. **(i) Expanded action space:** the agent is equipped with both a semantic `search` action  
198 for retrieving relevant pages and a novel `fetch` action for direct page access, enabling flexible ex-  
199 ploitation of document structure (§4.1). **(ii) Cross-level reward function:** supervision is provided  
200 jointly at the turn level and the token level, guiding the agent toward effective evidence collection  
201 and accurate answer generation (§4.2). **(iii) Visual semantic anchoring:** to stabilize RL training,  
202 ALDEN constrains the hidden-state evolution of generated and visual tokens respectively, mitigat-  
203 ing drift and preserving semantic grounding during optimization (§4.3). The overall RL training  
204 pipeline of ALDEN is illustrated in Fig. 2 and Alg. 1.

## 205 4.1 EXPANDED ACTION SPACE

206 In Agentic VRDU, agents must flexibly access information that may be referenced either semanti-  
207 cally or structurally. Relying solely on semantic retrieval is often insufficient: while it works for

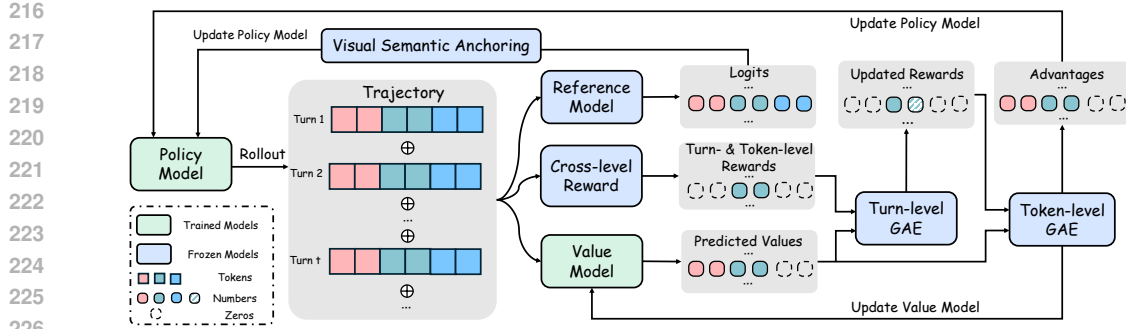


Figure 2: Overview of RL training in ALDEN. The policy model generates multi-turn trajectories, which are scored by a **cross-level reward function** and a **value model**. **Turn-level GAE** integrates future rewards to update the cross-level reward, and **token-level GAE** produces advantages for policy updates. A **reference model** supplies logits for both generated and visual tokens, which the **visual semantic anchoring** mechanism uses to constrain hidden-state evolution during optimization.

open-ended queries, it cannot efficiently resolve explicit page references (e.g., “see page 12”) or reasoning steps that span consecutive pages. To address this, ALDEN augments the standard `search` operation with a complementary `fetch` action, which enables direct page-index access and better exploits the inherent structure of documents. The action space thus consists of three options, each expressed in a structured format that combines free-form reasoning with explicit actions:

- **Search** — `<think>...</think><search>...</search>`  
Generates a reasoning trace within the `<think>` tags followed by a semantic query enclosed within the `<search>` tags. An external retrieval module returns a ranked list of pages relevant to the current query using semantic similarity. This action is effective for open-ended queries where relevant content is not explicitly referenced.
- **Fetch** — `<think>...</think><fetch>...</fetch>`  
Similar to search, but the agent specifies a page number within the `<fetch>` tag, enabling direct access to that page without semantic matching. This action is crucial for handling explicit references to page numbers or structured navigation across consecutive pages.
- **Answer** — `<think>...</think><answer>...</answer>`  
Outputs the reasoning trace followed by the final answer. This action terminates the rollout.

Once the action is parsed, the document returns the corresponding page images enclosed within the `<result>` tag. For the `search` action, the associated page numbers are also returned to provide cues of document structure.

#### 4.2 CROSS-LEVEL REWARD MODELING

Training agentic VRDU systems requires reward signals that are both structured enough to enforce valid behaviors and fine-grained enough to guide efficient exploration. To this end, ALDEN employs a cross-level reward function that integrates supervision at two complementary levels: turn-level rewards for overall action quality and token-level rewards for local shaping.

**Turn-level Reward.** The immediate turn-level reward  $r_t$  is defined as  $r_t = f_t + u_t$ , where the format reward  $f_t$  enforces the response format and the result reward  $u_t$  evaluates the quality of the action outcome. The format reward  $f_t$  is given by:

$$f_t = \begin{cases} 0, & \text{if the format is correct} \\ -1, & \text{otherwise} \end{cases} \quad (4)$$

Thus, only well-formed responses avoid penalty, ensuring consistent structured outputs across turns. The result reward is defined based on the action type  $a_t \in \{\text{search}, \text{fetch}, \text{answer}\}$ , the set of page indices collected in the current turn  $\mathcal{C}_t = \{c_1, \dots, c_{|\mathcal{C}_t|}\} \subseteq \{1, \dots, |\mathcal{D}|\}$ , the set of ground-truth page indices  $\mathcal{G} = \{g_1, \dots, g_{|\mathcal{G}|}\} \subseteq \{1, \dots, |\mathcal{D}|\}$ , and the set of previously accessed pages  $\mathcal{R} = \bigcup_{k=1}^{t-1} \mathcal{C}_k$ .

$$u_t = \mathbb{1}_{a_t=\text{answer}} \cdot \text{F1}(y, y') \cdot \alpha + \mathbb{1}_{a_t=\text{fetch}} \cdot (f_{\text{idx}}(\{c_1\}, \mathcal{G}) - f_{\text{rep}}(\mathcal{C}_t, \mathcal{R})) \cdot \eta + \mathbb{1}_{a_t=\text{search}} \cdot (NDCG@m - f_{\text{rep}}(\mathcal{C}_t, \mathcal{R})) \cdot \eta \quad (5)$$

270 where  $\mathbb{1}(\cdot)$  denotes the indicator function,  $\alpha > 1$  scales the reward of `answer` as the outcome  
 271 reward, and  $\eta$  controls the weight of the repetition penalty. The term  $\text{F1}(y, y')$  is the character-  
 272 level F1 score between the generated answer  $y'$  and the ground-truth answer  $y$ . For `fetch`,  
 273  $f_{idx}(\{c_1\}, \mathcal{G}) = e^{-\bar{d}(\{c_1\}, \mathcal{G})}$  smoothly rewards fetching pages near the ground-truth pages, where  
 274  $\bar{d}(i, \mathcal{G}) = \frac{1}{|\mathcal{G}|} \sum_{i=1}^{|\mathcal{G}|} |c_1 - g_i|$ .  $NDCG@m$  evaluates the ranked list of retrieved pages, providing  
 275 a fine-grained reward for search. For both `fetch` and `search`,  $f_{rep}(\mathcal{C}_t, \mathcal{R}) = \frac{|\mathcal{C}_t \cap \mathcal{R}|}{|\mathcal{C}_t|}$  penalizes  
 276 repeated page collection. To account for long-horizon credit assignment, following Zhou et al.  
 277 (2024); Wang et al. (2025a), we extend immediate rewards with turn-level GAE.  
 278

$$279 \hat{V}_t = \sum_{k=t}^T (\gamma_{\text{turn}} \lambda_{\text{turn}})^{k-t} \delta_k + V_\phi(s_t^L), \quad \delta_k = r_k + \gamma_{\text{turn}} V_\phi(s_{k+1}^L) - V_\phi(s_k^L) \quad (6)$$

282 where  $V_\phi(s_t^L)$  denotes the value predicted at the last token of the  $t$ -th response, serving as the turn-  
 283 level value estimate. The resulting  $\hat{V}_t$  replaces the raw  $r_t$  as the per-turn reward signal to provide a  
 284 richer learning signal that aligns token-level updates with long-horizon objectives.

285 **Token-level Reward.** Unlike the `fetch` action, whose argument is a single page number, the  
 286 `search` action takes a search query composed of multiple tokens. A turn-level repetition penalty  
 287 cannot identify which tokens are repeated, and thus fails to effectively curb redundant search actions.  
 288 To address this limitation, we further introduce a token-level penalty applied specifically to the query  
 289 span of search actions. Starting from the second invocation of `search` within an episode, we compute  
 290 the maximum Jaccard similarity between the current query's n-grams and those of all past queries:

$$291 \text{overlap}_t = \max_{j < t} \frac{|Q_n(q_t) \cap Q_n(q_j)|}{|Q_n(q_t) \cup Q_n(q_j)|} \quad (7)$$

293 where  $Q_n(q)$  denotes the set of n-grams of the query. To distribute this penalty at the token level,  
 294 we assign per-token weights so that tokens inside repeated n-grams receive proportionally higher  
 295 penalties. For each token  $u$  in the query span  $a_t^{\text{query}}$ , the weight is defined as  $w_u = \frac{c_u}{\sum_{v \in a_t^{\text{query}}} c_v}$ ,  
 296 where  $c_u \in \{0, 1, 2, \dots\}$  counts how many repeated n-grams include token  $u$ .

297 Finally, the reward assigned to each generated token  $a_t^i$  within turn  $t$  is defined by combining turn-  
 298 level and token-level signals:

$$300 r_t^i = \begin{cases} \hat{V}_t, & \text{if } i = L \\ 301 -w_i \cdot \text{overlap}_t, & \text{if } t > 1 \text{ and } a_t = \text{search} \text{ and } a_t^i \in a_t^{\text{query}} \\ 302 0, & \text{otherwise} \end{cases} \quad (8)$$

303 This formulation anchors the turn-level objective to the response boundary, while applying localized  
 304 penalties to redundant query tokens, yielding a unified cross-level reward signal for token-level PPO  
 305 training. Token-level GAE is then applied to compute advantages for policy updates as in Eq. (2).

### 307 4.3 VISUAL SEMANTIC ANCHORING

309 A unique challenge in RL training for A-VRDU stems from the large number of visual tokens in  
 310 the trajectory introduced by high-resolution document pages. Without explicit constraints on these  
 311 tokens, we empirically observe pronounced training fluctuations and rapid entropy collapse (Fig. 3).  
 312 To address this issue, we propose a Visual Semantic Anchoring mechanism that constrains hidden  
 313 states during policy optimization through dual-path KL regularization. The KL term for textual  
 314 tokens regularizes the policy distribution against a frozen reference model, stabilizing language  
 315 generation, while the KL term for visual tokens anchors their hidden states to the reference model,  
 316 preserving semantic grounding and preventing drift. Formally, we define

$$317 \mathcal{L}_{\text{policy}} = \mathbb{E}_x \left[ \frac{1}{T} \sum_{t=1}^T \left[ \frac{1}{L} \sum_{i=1}^L \left[ \min \left[ \frac{\pi_\theta(a_t^i | s_t^i)}{\pi_{\text{old}}(a_t^i | s_t^i)} A_t^i, \text{clip} \left( \frac{\pi_\theta(a_t^i | s_t^i)}{\pi_{\text{old}}(a_t^i | s_t^i)}, 1 - \epsilon, 1 + \epsilon \right) A_t^i \right] \right] \right. \right. \\ 318 \left. \left. + \beta_{\text{gen}} \text{KL}[\pi_\theta(a_t^i | s_t^i) || \pi_{\text{ref}}(a_t^i | s_t^i)] + \frac{1}{H} \sum_{j=1}^H \beta_{\text{obs}} \text{KL}[\pi_\theta(o_t^j | o_t^{<j}, a_t, s_t) || \pi_{\text{ref}}(o_t^j | o_t^{<j}, a_t, s_t)] \right] \right] \quad (9)$$

322 where  $H$  denotes the number of visual tokens.  $\beta_{\text{gen}}$  and  $\beta_{\text{obs}}$  are independent coefficients. In practice,  
 323 we set  $\beta_{\text{obs}} > \beta_{\text{gen}}$  to tightly regularize the much larger observation-token set while allowing more  
 324 flexibility for generated tokens to adapt to the task.

324 

## 5 EXPERIMENTS

326 We conduct experiments on long VRDU benchmarks to (i) compare ALDEN with strong baselines  
 327 and (ii) assess the contribution of its key components, including expanded action space, cross-level  
 328 reward, and visual semantic anchoring, to navigation accuracy, answer quality, and training stabil-  
 329 ity. We first outline datasets, baselines, implementation details, and evaluation metrics (§5.1), then  
 330 present main results (§5.2), followed by ablations (§5.3) and detailed component analyses (§5.4).

332 

### 5.1 EXPERIMENTAL SETUP

334 **Datasets.** We build the training set by merging and processing three multi-page  
 335 VRDU datasets: DUDE (Van Landeghem et al., 2023), MPDocVQA (Tito et al., 2023a),  
 336 and SlideVQA (Tanaka et al., 2023a). We filter out documents with fewer than 10  
 337 pages. To enrich query diversity, we use GPT-4o (Hurst et al., 2024) to rewrite part  
 338 of MPDocVQA, increasing the proportion of page-index-referenced queries in the final  
 339 training corpus. Detailed statistics of the resulting training set are provided in Tab. 1.  
 340 The evaluation is conducted mainly on  
 341 the following VRDU benchmarks: **MM-LongBench** (Ma et al., 2024b), **Long-  
 342 DocURL** (Deng et al., 2024), **PaperTab** (Hui et al., 2024), **PaperText** (Hui  
 343 et al., 2024), and **FetaTab** (Hui et al., 2024). To evaluate the `fetch` action,  
 344 we create DUDE-sub, a DUDE validation  
 345 subset with 480 general queries and 480 queries containing explicit page references or implicit se-  
 346 quential navigation cues. More details about the dataset can be seen in Appx. A.

347 Table 1: Statistics of the training dataset. #GQ and  
 348 #PQ denote the numbers of general user queries and page-  
 349 index-referenced queries, respectively.

Sub-dataset	DUDE	SlideVQA	MPDocVQA
#GQ	6,943	10,615	7,992
#PQ	1,011	2	4,165
Sum	7,954	10,617	12,157

350 **Baselines.** To validate the effectiveness of ALDEN, we compare it with three categories of base-  
 351 lines. (1) **Full-Document Input**: mainstream state-of-the-art VLMs are prompted with the entire  
 352 document as context to answer user queries. (2) **Visual RAG**: methods that retrieve the most relevant  
 353 document pages using the user query, including M3DocRAG (Cho et al., 2024), and ReSearch-VL,  
 354 a Search-only ALDEN variant trained with GRPO using outcome-based rewards adapted from a  
 355 fully textual method ReSearch (Chen et al., 2025b). (3) **Hybrid RAG**: approaches that augment  
 356 page images with OCR-extracted text for retrieval and reasoning, including MDocAgent (Han et al.,  
 357 2025), VidoRAG (Wang et al., 2025b). Detailed baseline configurations can be seen in Appx. B

358 **Implementation Details.** Both the policy and value models are initialized from Qwen2.5-VL-7B-  
 359 Instruct (Bai et al., 2025), and all Visual RAG and Hybrid RAG baselines use the same backbone  
 360 for fairness. During training, we adopt the single-vector retriever vdr-2b-v1 (Ma et al., 2024a) for  
 361 images and e5-large-v2 (Wang et al., 2022) for text. For evaluation, we also report results with the  
 362 multi-vector retrievers ColQwen2-v1.0 (ColQwen) (Faysse et al., 2025) for images and ColBERT-  
 363 v2.0 (ColBERT) (Santhanam et al., 2021) for text. Unless otherwise noted, each `search` action  
 364 retrieves the top-1 candidate page, with a maximum of  $T = 6$  reasoning-action turns. On average,  
 365 ALDEN collects 1.87 unique pages per query; hence, single-turn RAG baselines are set to retrieve  
 366 the top-2 pages for a fair comparison. Further implementation details are provided in Appx. C.

367 **Evaluation Metrics.** The primary evaluation metric is GPT-4o-judged answer accuracy (**Acc**) on  
 368 each benchmark. For finer-grained analysis of ALDEN’s components, we further assess navigation  
 369 quality using trajectory-level retrieval recall (**Rec**), precision (**Pre**), F1-score (**F1**), and the number  
 370 of unique collected pages (**#UP**). Detailed definitions of these metrics are provided in Appx. D.

371 

### 5.2 MAIN RESULTS

372 Table 5.2 reports answer accuracy across all baselines. Directly prompting large VLMs with the  
 373 entire document performs poorly ( $\text{Acc} < 0.30$ ), confirming the difficulty of long-document reasoning  
 374 where irrelevant content overwhelms true evidence. Retrieval-based methods achieve substantially  
 375 better results. Among Visual RAG approaches, ALDEN with ColQwen attains the highest average  
 376 accuracy (0.410), surpassing M3DocRAG by 3.2 points. In Hybrid RAG, baselines such as Vi-  
 377 DoRAG and MDdocAgent benefit from textual signals but are limited by fixed reasoning pipelines.  
 ALDEN with hybrid retrievers achieves the best overall performance, exceeding the strongest hy-

378

379  
380  
Table 2: Answer accuracy comparison on five VRDU benchmarks.  $\dagger$  indicates the strongest non-ALDEN  
baseline used to compute the relative improvement (%). **Bold** indicates the best result per dataset.

Method	MMLongBench	LongDocUrl	PaperTab	PaperText	FetaTab	Avg
<i>Full Document Input</i>						
SmolVLM-Instruct (Marafioti et al.)	0.072	0.165	0.065	0.142	0.148	0.118
Phi-3.5-Vision-Instruct (Abdin et al.)	0.141	0.285	0.068	0.174	0.232	0.180
mPLUG-DocOwl2 (Hu et al.)	0.159	0.273	0.072	0.162	0.288	0.191
Qwen2-VL-7B-Instruct (Wang et al.)	0.177	0.280	0.077	0.146	0.339	0.203
LEOPARD (Jia et al.)	0.196	0.313	0.112	0.189	0.341	0.230
Qwen2.5-VL-7B-Instruct (Bai et al.)	0.221	0.375	0.131	0.265	0.336	0.265
InternVL3.5-8B-Instruct (Wang et al.)	0.219	0.381	0.130	0.271	0.348	0.270
<i>Visual RAG methods</i>						
ReSearch-VL (ColQwen)	0.274	0.384	0.150	0.295	0.406	0.302
M3DocRAG (ColQwen) $\dagger$	0.330	0.464	0.201	0.350	0.547	0.378
<b>ALDEN</b> (vdr-2b-v1)	0.335	0.513	0.201	0.342	0.542	0.386
<b>ALDEN</b> (ColQwen)	0.367	0.526	0.211	0.345	0.603	0.410
Relative Improvement (%)	11.21	13.36	4.98	-1.43	10.23	10.81
<i>Hybrid RAG methods</i>						
ViDoRAG (ColQwen + CoBERT)	0.215	0.323	0.158	0.264	0.358	0.264
MDocAgent (ColQwen + CoBERT) $\dagger$	0.347	0.494	0.221	0.408	0.607	0.415
<b>ALDEN</b> (vdr-2b-v1 + c5-large-v2)	0.385	0.542	0.228	0.416	0.611	0.436
<b>ALDEN</b> (ColQwen + CoBERT)	<b>0.392</b>	<b>0.551</b>	<b>0.245</b>	<b>0.421</b>	<b>0.623</b>	<b>0.446</b>
Relative Improvement (%)	12.97	11.54	10.86	3.18	2.63	7.47

396  
397  
Table 3: Answer accuracy for different ablations of ALDEN on five VRDU benchmarks. **Bold** indicates the  
best result per dataset.

Method	MMLongBench	LongDocUrl	PaperTab	PaperText	FetaTab	Avg
Full ALDEN	<b>0.335</b>	<b>0.513</b>	<b>0.201</b>	<b>0.342</b>	<b>0.542</b>	<b>0.386</b>
w/o Fetch	0.301	0.469	0.140	0.258	0.443	0.322
w/o Cross-level Reward	0.329	0.483	0.148	0.301	0.518	0.356
w/o Visual Semantic Anchoring	0.326	0.502	0.181	0.328	0.529	0.373

403  
404  
405  
406  
407  
408  
409  
410  
411  
412  
413  
414  
415  
416  
417  
418  
419  
420  
421  
422  
423  
424  
425  
426  
427  
428  
429  
430  
431  
432  
433  
434  
435  
436  
437  
438  
439  
440  
441  
442  
443  
444  
445  
446  
447  
448  
449  
450  
451  
452  
453  
454  
455  
456  
457  
458  
459  
460  
461  
462  
463  
464  
465  
466  
467  
468  
469  
470  
471  
472  
473  
474  
475  
476  
477  
478  
479  
480  
481  
482  
483  
484  
485  
486  
487  
488  
489  
490  
491  
492  
493  
494  
495  
496  
497  
498  
499  
500  
501  
502  
503  
504  
505  
506  
507  
508  
509  
510  
511  
512  
513  
514  
515  
516  
517  
518  
519  
520  
521  
522  
523  
524  
525  
526  
527  
528  
529  
530  
531  
532  
533  
534  
535  
536  
537  
538  
539  
540  
541  
542  
543  
544  
545  
546  
547  
548  
549  
550  
551  
552  
553  
554  
555  
556  
557  
558  
559  
560  
561  
562  
563  
564  
565  
566  
567  
568  
569  
570  
571  
572  
573  
574  
575  
576  
577  
578  
579  
580  
581  
582  
583  
584  
585  
586  
587  
588  
589  
590  
591  
592  
593  
594  
595  
596  
597  
598  
599  
600  
601  
602  
603  
604  
605  
606  
607  
608  
609  
610  
611  
612  
613  
614  
615  
616  
617  
618  
619  
620  
621  
622  
623  
624  
625  
626  
627  
628  
629  
630  
631  
632  
633  
634  
635  
636  
637  
638  
639  
640  
641  
642  
643  
644  
645  
646  
647  
648  
649  
650  
651  
652  
653  
654  
655  
656  
657  
658  
659  
660  
661  
662  
663  
664  
665  
666  
667  
668  
669  
670  
671  
672  
673  
674  
675  
676  
677  
678  
679  
680  
681  
682  
683  
684  
685  
686  
687  
688  
689  
690  
691  
692  
693  
694  
695  
696  
697  
698  
699  
700  
701  
702  
703  
704  
705  
706  
707  
708  
709  
710  
711  
712  
713  
714  
715  
716  
717  
718  
719  
720  
721  
722  
723  
724  
725  
726  
727  
728  
729  
730  
731  
732  
733  
734  
735  
736  
737  
738  
739  
740  
741  
742  
743  
744  
745  
746  
747  
748  
749  
750  
751  
752  
753  
754  
755  
756  
757  
758  
759  
760  
761  
762  
763  
764  
765  
766  
767  
768  
769  
770  
771  
772  
773  
774  
775  
776  
777  
778  
779  
780  
781  
782  
783  
784  
785  
786  
787  
788  
789  
790  
791  
792  
793  
794  
795  
796  
797  
798  
799  
800  
801  
802  
803  
804  
805  
806  
807  
808  
809  
810  
811  
812  
813  
814  
815  
816  
817  
818  
819  
820  
821  
822  
823  
824  
825  
826  
827  
828  
829  
830  
831  
832  
833  
834  
835  
836  
837  
838  
839  
840  
841  
842  
843  
844  
845  
846  
847  
848  
849  
850  
851  
852  
853  
854  
855  
856  
857  
858  
859  
860  
861  
862  
863  
864  
865  
866  
867  
868  
869  
870  
871  
872  
873  
874  
875  
876  
877  
878  
879  
880  
881  
882  
883  
884  
885  
886  
887  
888  
889  
889  
890  
891  
892  
893  
894  
895  
896  
897  
898  
899  
900  
901  
902  
903  
904  
905  
906  
907  
908  
909  
910  
911  
912  
913  
914  
915  
916  
917  
918  
919  
920  
921  
922  
923  
924  
925  
926  
927  
928  
929  
930  
931  
932  
933  
934  
935  
936  
937  
938  
939  
940  
941  
942  
943  
944  
945  
946  
947  
948  
949  
950  
951  
952  
953  
954  
955  
956  
957  
958  
959  
960  
961  
962  
963  
964  
965  
966  
967  
968  
969  
970  
971  
972  
973  
974  
975  
976  
977  
978  
979  
980  
981  
982  
983  
984  
985  
986  
987  
988  
989  
989  
990  
991  
992  
993  
994  
995  
996  
997  
998  
999  
1000  
1001  
1002  
1003  
1004  
1005  
1006  
1007  
1008  
1009  
10010  
10011  
10012  
10013  
10014  
10015  
10016  
10017  
10018  
10019  
10020  
10021  
10022  
10023  
10024  
10025  
10026  
10027  
10028  
10029  
10030  
10031  
10032  
10033  
10034  
10035  
10036  
10037  
10038  
10039  
10040  
10041  
10042  
10043  
10044  
10045  
10046  
10047  
10048  
10049  
10050  
10051  
10052  
10053  
10054  
10055  
10056  
10057  
10058  
10059  
10060  
10061  
10062  
10063  
10064  
10065  
10066  
10067  
10068  
10069  
10070  
10071  
10072  
10073  
10074  
10075  
10076  
10077  
10078  
10079  
10080  
10081  
10082  
10083  
10084  
10085  
10086  
10087  
10088  
10089  
10090  
10091  
10092  
10093  
10094  
10095  
10096  
10097  
10098  
10099  
100100  
100101  
100102  
100103  
100104  
100105  
100106  
100107  
100108  
100109  
100110  
100111  
100112  
100113  
100114  
100115  
100116  
100117  
100118  
100119  
100120  
100121  
100122  
100123  
100124  
100125  
100126  
100127  
100128  
100129  
100130  
100131  
100132  
100133  
100134  
100135  
100136  
100137  
100138  
100139  
100140  
100141  
100142  
100143  
100144  
100145  
100146  
100147  
100148  
100149  
100150  
100151  
100152  
100153  
100154  
100155  
100156  
100157  
100158  
100159  
100160  
100161  
100162  
100163  
100164  
100165  
100166  
100167  
100168  
100169  
100170  
100171  
100172  
100173  
100174  
100175  
100176  
100177  
100178  
100179  
100180  
100181  
100182  
100183  
100184  
100185  
100186  
100187  
100188  
100189  
100190  
100191  
100192  
100193  
100194  
100195  
100196  
100197  
100198  
100199  
100200  
100201  
100202  
100203  
100204  
100205  
100206  
100207  
100208  
100209  
100210  
100211  
100212  
100213  
100214  
100215  
100216  
100217  
100218  
100219  
100220  
100221  
100222  
100223  
100224  
100225  
100226  
100227  
100228  
100229  
100230  
100231  
100232  
100233  
100234  
100235  
100236  
100237  
100238  
100239  
100240  
100241  
100242  
100243  
100244  
100245  
100246  
100247  
100248  
100249  
100250  
100251  
100252  
100253  
100254  
100255  
100256  
100257  
100258  
100259  
100260  
100261  
100262  
100263  
100264  
100265  
100266  
100267  
100268  
100269  
100270  
100271  
100272  
100273  
100274  
100275  
100276  
100277  
100278  
100279  
100280  
100281  
100282  
100283  
100284  
100285  
100286  
100287  
100288  
100289  
100290  
100291  
100292  
100293  
100294  
100295  
100296  
100297  
100298  
100299  
100300  
100301  
100302  
100303  
100304  
100305  
100306  
100307  
100308  
100309  
100310  
100311  
100312  
100313  
100314  
100315  
100316  
100317  
100318  
100319  
100320  
100321  
100322  
100323  
100324  
100325  
100326  
100327  
100328  
100329  
100330  
100331  
100332  
100333  
100334  
100335  
100336  
100337  
100338  
100339  
100340  
100341  
100342  
100343  
100344  
100345  
100346  
100347  
100348  
100349  
100350  
100351  
100352  
100353  
100354  
100355  
100356  
100357  
100358  
100359  
100360  
100361  
100362  
100363  
100364  
100365  
100366  
100367  
100368  
100369  
100370  
100371  
100372  
100373  
100374  
100375  
100376  
100377  
100378  
100379  
100380  
100381  
100382  
100383  
100384  
100385  
100386  
100387  
100388  
100389  
100390  
100391  
100392  
100393  
100394  
100395  
100396  
100397  
100398  
100399  
100400  
100401  
100402  
100403  
100404  
100405  
100406  
100407  
100408  
100409  
100410  
100411  
100412  
100413  
100414  
100415  
100416  
100417  
100418  
100419  
100420  
100421  
100422  
100423  
100424  
100425  
100426  
100427  
100428  
100429  
100430  
100431  
100432  
100433  
100434  
100435  
100436  
100437  
100438  
100439  
100440  
100441  
100442  
100443  
100444  
100445  
100446  
100447  
100448  
100449  
100450  
100451  
100452  
100453  
100454  
100455  
100456  
100457  
100458  
100459  
100460  
100461  
100462  
100463  
100464  
100465  
100466  
100467  
100468  
100469  
100470  
100471  
100472  
100473  
100474  
100475  
100476  
100477  
100478  
100479  
100480  
100481  
100482  
100483  
100484  
100485  
100486  
100487  
100488  
100489  
100490  
100491  
100492  
100493  
100494  
100495  
100496  
100497  
100498  
100499  
100500  
100501  
100502  
100503  
100504  
100505  
100506  
100507  
100508  
100509  
100510  
100511  
100512  
100513  
100514  
100515  
100516  
100517  
100518  
100519  
100520  
100521  
100522  
100523  
100524  
100525  
100526  
100527  
100528  
100529  
100530  
100531  
100532  
100533  
100534  
100535  
100536  
100537  
100538  
100539  
100540  
100541  
100542  
100543  
100544  
100545  
100546  
100547  
100548  
100549  
100550  
100551  
100552  
100553  
100554  
100555  
100556  
100557  
100558  
100559  
100560  
100561  
100562  
100563  
100564  
100565  
100566  
100567  
100568  
100569  
100570  
100571  
100572  
100573  
100574  
100575  
100576  
100577  
100578  
100579  
100580  
100581  
100582  
100583  
100584  
100585  
100586  
100587  
100588  
100589  
100590  
100591  
100592  
100593  
100594  
100595  
100596  
100597  
100598  
100599  
100600  
100601  
100602  
100603  
100604  
100605  
100606  
100607  
100608  
100609  
100610  
100611  
100612  
100613  
100614  
100615  
100616  
100617  
100618  
100619  
100620  
100621  
100622  
100623  
100624  
100625  
100626  
100627  
100628  
100629  
100630  
100631  
100632  
100633  
100634  
100635  
100636  
100637  
100638  
100639  
100640  
100641  
100642  
100643  
100644  
100645  
100646  
100647  
100648  
100649  
100650  
100651  
100652  
100653  
100654  
100655  
100656  
100657  
100658  
100659  
100660  
100661  
100662  
100663  
100664  
100665  
100666  
100667  
100668  
100669  
100670  
100671  
100672  
100673  
100674  
100675  
100676  
100677  
100678  
100679  
100680  
100681  
100682  
100683  
100684  
100685  
100686  
100687  
100688  
100689  
100690  
100691  
100692  
100693  
100694  
100695  
100696  
100697  
100698  
1006

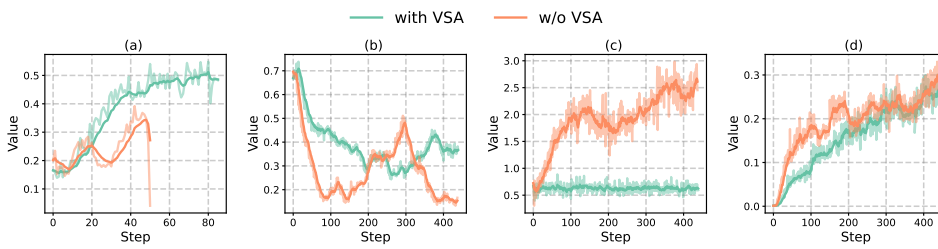


Figure 3: Training dynamics of ALDEN with and without Visual Semantic Anchoring (VSA). Panel (a) shows the turn-level reward of the `answer` action, panel (b) shows token-level entropy, panel (c) and (d) plot the KL divergence of visual tokens and generated tokens respectively.

The number of unique pages rises from 1.03 to 1.19, reflecting broader coverage. These results confirm that combining index-based `fetch` with semantic search enables more flexible and efficient navigation, especially for queries that reference specific pages or require traversal across consecutive pages.

**Effect of Reward Design.** We evaluate how different reward schemes affect ALDEN’s retrieval and reasoning (Table 5). (i) Outcome-based Only assigns a single scalar reward for final answer correctness. (ii) Turn-level + Outcome adds rule-based turn-level supervision, improving Acc from 0.483 to 0.509 and Rec from 0.483 to 0.497, showing that denser feedback aids evidence localization. (iii) Full ALDEN further introduces token-level shaping, yielding a smaller but consistent gain (Acc 0.513, Rec 0.506) and increasing unique pages from 1.22 to 1.39, indicating reduced query repetition and broader exploration. Overall, the cross-level reward design fosters richer query reformulation and more thorough evidence gathering, enhancing both navigation and answer quality.

**Effect of Visual Semantic Anchoring.** We evaluate the effect of Visual Semantic Anchoring (VSA) on training stability and representation drift, as shown in Figure 3. With a larger batch size (512) than in the main experiments (128), the VSA-enabled model achieves steadily increasing answer rewards, while the non-VSA variant fluctuates and collapses (a). VSA also maintains higher policy entropy, supporting healthier exploration (b). For representation alignment, KL divergence of visual tokens grows unchecked without VSA, indicating hidden-state drift, whereas VSA constrains these values while allowing moderate growth for action tokens (c,d). Overall, VSA achieves stabilizing RL training and preventing drift in visual representations.

Table 4: Comparison between search-only and full ALDEN on the DUDE-sub dataset.

Method	Acc	Rec	Pre	F1	#UP
Search-only	0.545	0.471	0.841	0.531	1.03
Full ALDEN	<b>0.653</b>	<b>0.598</b>	<b>0.874</b>	<b>0.628</b>	<b>1.19</b>

Table 5: Effect of reward design of outcome-based, turn-level and outcome-based, and full ALDEN on LongDocURL.

Method	Acc	Rec	Pre	F1	#UP
Outcome-based Only	0.483	0.483	0.612	0.520	1.27
Turn-level + Outcome	0.509	0.497	0.608	0.522	1.22
Full ALDEN	<b>0.513</b>	<b>0.506</b>	<b>0.612</b>	<b>0.526</b>	<b>1.39</b>

## 6 CONCLUSIONS

We introduced the **Agentic VRDU** task and proposed **ALDEN**, a reinforcement-learning framework that trains VLMs as autonomous agents capable of multi-turn navigation and evidence gathering. ALDEN integrates a `fetch` action for direct page access, a cross-level reward for fine-grained reward modeling, and a visual semantic anchoring mechanism for stable training. Extensive experiments on multiple long-document benchmarks show that ALDEN achieves state-of-the-art accuracy and improves evidence localization. Ablation studies further confirm the contribution of each component and offer broader insights for multi-turn RL in multimodal agents. The A-VRDU paradigm marks a shift from passive document reading to autonomous navigation and reasoning across vast information landscapes, and ALDEN’s strong performance demonstrates the potential of such agents to deliver more accurate, scalable, and adaptive understanding of complex, visually rich documents. While promising, the trained agent still faces challenges in balancing exploration and exploitation and in reliably recognizing true evidence pages. Future work could focus on building larger and higher-quality datasets, leveraging trajectories from stronger models with validation and reflection, and adopting curriculum learning to handle tasks of varying difficulty.

486 LLM USAGE STATEMENT  
487488 Large Language Models (LLMs) were used as general-purpose writing and editing aids. Specifi-  
489 cally, OpenAI’s ChatGPT (GPT-5) assisted in polishing grammar, improving clarity, and suggesting  
490 alternative phrasings. All research ideas, experimental design, data processing, model development,  
491 and analysis were conceived and executed solely by the authors. The LLM provided no novel re-  
492 search insights or substantive scientific contributions.494 REPRODUCIBILITY STATEMENT  
495496 We are committed to ensuring the reproducibility of our results. To this end, we will release:  
497498 • All source code for training, evaluation, and data preprocessing, including scripts for dataset con-  
499 struction, reward computation, and reinforcement-learning training with ALDEN.  
500 • The processed training corpus derived from DUDE, MPDocVQA, and SlideVQA, along with  
501 instructions to regenerate it from the original public datasets.  
502 • Detailed configuration files specifying model hyperparameters, random seeds, and hardware set-  
503 tings.  
504 • Checkpoints for both the policy and value models, and prompts used for GPT-4o evaluation.505 Our experiments were run on NVIDIA A100 GPUs (80GB) with PyTorch 2.4 and HuggingFace  
506 Transformers 4.49; exact package versions will be provided in the released code. These resources  
507 will allow other researchers to fully reproduce our training, evaluation, and analysis results.  
508510 REFERENCES  
511512 Marah Abdin, Jyoti Aneja, Harkirat Behl, Sébastien Bubeck, Ronen Eldan, Suriya Gunasekar,  
513 Michael Harrison, Russell J Hewett, Mojan Javaheripi, Piero Kauffmann, et al. Phi-4 techni-  
514 cal report. *arXiv preprint arXiv:2412.08905*, 2024.516 Shuai Bai, Keqin Chen, Xuejing Liu, Jialin Wang, Wenbin Ge, Sibo Song, Kai Dang, Peng Wang,  
517 Shijie Wang, Jun Tang, et al. Qwen2. 5-vl technical report. *arXiv preprint arXiv:2502.13923*,  
518 2025.519 Richard Bellman. A markovian decision process. *Journal of mathematics and mechanics*, pp. 679–  
520 684, 1957.522 Tsachi Blau, Sharon Fogel, Roi Ronen, Alona Golts, Roy Ganz, Elad Ben Avraham, Aviad Aber-  
523 dam, Shahar Tsiper, and Ron Litman. Gram: Global reasoning for multi-page vqa. In *Proceedings*  
524 of the IEEE/CVF Conference on Computer Vision and Pattern Recognition, pp. 15598–15607,  
525 2024.526 Jian Chen, Ruiyi Zhang, Yufan Zhou, Tong Yu, Franck Dernoncourt, Jiuxiang Gu, Ryan A. Rossi,  
527 Changyou Chen, and Tong Sun. SV-RAG: LoRA-contextualizing adaptation of MLLMs for long  
528 document understanding. In *The Thirteenth International Conference on Learning Representa-  
529 tions*, 2025a. URL <https://openreview.net/forum?id=FDaHjwInXO>.531 Mingyang Chen, Tianpeng Li, Haoze Sun, Yijie Zhou, Chenzheng Zhu, Haofen Wang, Jeff Z Pan,  
532 Wen Zhang, Huajun Chen, Fan Yang, et al. Learning to reason with search for llms via reinfor-  
533 cement learning. *arXiv preprint arXiv:2503.19470*, 2025b.534 Jaemin Cho, Debanjan Mahata, Ozan Irsoy, Yujie He, and Mohit Bansal. M3docrag: Multi-  
535 modal retrieval is what you need for multi-page multi-document understanding. *arXiv preprint  
536 arXiv:2411.04952*, 2024.538 Chao Deng, Jiale Yuan, Pi Bu, Peijie Wang, Zhong-Zhi Li, Jian Xu, Xiao-Hui Li, Yuan Gao, Jun  
539 Song, Bo Zheng, et al. Longdocurl: a comprehensive multimodal long document benchmark  
integrating understanding, reasoning, and locating. *arXiv preprint arXiv:2412.18424*, 2024.

540 Yihao Ding, Zhe Huang, Runlin Wang, YanHang Zhang, Xianru Chen, Yuzhong Ma, Hyunsuk  
 541 Chung, and Soyeon Caren Han. V-doc: Visual questions answers with documents. In *Proceedings*  
 542 *of the IEEE/CVF conference on computer vision and pattern recognition*, pp. 21492–21498, 2022.  
 543

544 Manuel Faysse, Hugues Sibille, Tony Wu, Bilel Omrani, Gautier Viaud, CELINE HUDELOT,  
 545 and Pierre Colombo. Colpali: Efficient document retrieval with vision language models. In  
 546 *The Thirteenth International Conference on Learning Representations*, 2025. URL <https://openreview.net/forum?id=ogjBpZ8uSi>.  
 547

548 Hao Feng, Qi Liu, Hao Liu, Jingqun Tang, Wengang Zhou, Houqiang Li, and Can Huang. Docpedia:  
 549 Unleashing the power of large multimodal model in the frequency domain for versatile document  
 550 understanding. *Science China Information Sciences*, 67(12):1–14, 2024.  
 551

552 Siwei Han, Peng Xia, Ruiyi Zhang, Tong Sun, Yun Li, Hongtu Zhu, and Huaxiu Yao. Mdoca-  
 553 gent: A multi-modal multi-agent framework for document understanding. *arXiv preprint*  
 554 *arXiv:2503.13964*, 2025.  
 555

556 Anwen Hu, Haiyang Xu, Liang Zhang, Jiabo Ye, Ming Yan, Ji Zhang, Qin Jin, Fei Huang, and  
 557 Jingren Zhou. mplug-docowl2: High-resolution compressing for ocr-free multi-page document  
 558 understanding. *arXiv preprint arXiv:2409.03420*, 2024.  
 559

560 Yulong Hui, Yao Lu, and Huanchen Zhang. Uda: A benchmark suite for retrieval augmented gener-  
 561 ation in real-world document analysis. *Advances in Neural Information Processing Systems*, 37:  
 562 67200–67217, 2024.  
 563

564 Aaron Hurst, Adam Lerer, Adam P Goucher, Adam Perelman, Aditya Ramesh, Aidan Clark, AJ Os-  
 565 trow, Akila Welihinda, Alan Hayes, Alec Radford, et al. Gpt-4o system card. *arXiv preprint*  
 566 *arXiv:2410.21276*, 2024.  
 567

568 Mengzhao Jia, Wenhao Yu, Kaixin Ma, Tianqing Fang, Zhihan Zhang, Siru Ouyang, Hongming  
 569 Zhang, Dong Yu, and Meng Jiang. Leopard: A vision language model for text-rich multi-image  
 570 tasks. *arXiv preprint arXiv:2410.01744*, 2024.  
 571

572 Bowen Jin, Hansi Zeng, Zhenrui Yue, Jinsung Yoon, Sercan Arik, Dong Wang, Hamed Zamani, and  
 573 Jiawei Han. Search-r1: Training llms to reason and leverage search engines with reinforce-  
 574 learning. *arXiv preprint arXiv:2503.09516*, 2025.  
 575

576 Bo Li, Yuanhan Zhang, Dong Guo, Renrui Zhang, Feng Li, Hao Zhang, Kaichen Zhang, Peiyuan  
 577 Zhang, Yanwei Li, Ziwei Liu, et al. Llava-onevision: Easy visual task transfer. *arXiv preprint*  
 578 *arXiv:2408.03326*, 2024.  
 579

580 Zhenwen Liang, Kehan Guo, Gang Liu, Taicheng Guo, Yujun Zhou, Tianyu Yang, Jiajun Jiao,  
 581 Renjie Pi, Jipeng Zhang, and Xiangliang Zhang. SceMQA: A scientific college entrance level  
 582 multimodal question answering benchmark. In Lun-Wei Ku, Andre Martins, and Vivek Sriku-  
 583 mar (eds.), *Proceedings of the 62nd Annual Meeting of the Association for Computational*  
 584 *Linguistics (Volume 2: Short Papers)*, pp. 109–119, Bangkok, Thailand, August 2024. Asso-  
 585 ciation for Computational Linguistics. doi: 10.18653/v1/2024.acl-short.11. URL <https://aclanthology.org/2024.acl-short.11/>.  
 586

587 Haotian Liu, Chunyuan Li, Yuheng Li, and Yong Jae Lee. Improved baselines with visual instruction  
 588 tuning. In *Proceedings of the IEEE/CVF conference on computer vision and pattern recognition*,  
 589 pp. 26296–26306, 2024a.  
 590

591 Yuliang Liu, Biao Yang, Qiang Liu, Zhang Li, Zhiyin Ma, Shuo Zhang, and Xiang Bai.  
 592 Textmonkey: An ocr-free large multimodal model for understanding document. *arXiv preprint*  
 593 *arXiv:2403.04473*, 2024b.  
 594

595 Tengchao Lv, Yupan Huang, Jingye Chen, Yuzhong Zhao, Yilin Jia, Lei Cui, Shuming Ma, Yaoyao  
 596 Chang, Shaohan Huang, Wenhui Wang, et al. Kosmos-2.5: A multimodal literate model. *arXiv*  
 597 *preprint arXiv:2309.11419*, 2023.  
 598

594 Xueguang Ma, Sheng-Chieh Lin, Minghan Li, Wenhui Chen, and Jimmy Lin. Unifying multi-  
 595 modal retrieval via document screenshot embedding. In Yaser Al-Onaizan, Mohit Bansal, and  
 596 Yun-Nung Chen (eds.), *Proceedings of the 2024 Conference on Empirical Methods in Natu-  
 597 ral Language Processing*, pp. 6492–6505, Miami, Florida, USA, November 2024a. Associa-  
 598 tion for Computational Linguistics. doi: 10.18653/v1/2024.emnlp-main.373. URL <https://aclanthology.org/2024.emnlp-main.373/>.

600 Yubo Ma, Yuhang Zang, Liangyu Chen, Meiqi Chen, Yizhu Jiao, Xinze Li, Xinyuan Lu, Ziyu  
 601 Liu, Yan Ma, Xiaoyi Dong, Pan Zhang, Liangming Pan, Yu-Gang Jiang, Jiaqi Wang, Yixin Cao,  
 602 and Aixin Sun. MMLONGBENCH-DOC: Benchmarking long-context document understand-  
 603 ing with visualizations. In *The Thirty-eight Conference on Neural Information Processing Systems  
 604 Datasets and Benchmarks Track*, 2024b. URL <https://openreview.net/forum?id=1oJM1acwzf>.

606 Andrés Marafioti, Orr Zohar, Miquel Farré, Merve Noyan, Elie Bakouch, Pedro Manuel Cuenca  
 607 Jiménez, Cyril Zakka, Loubna Ben allal, Anton Lozhkov, Nouamane Tazi, Vaibhav Srivas-  
 608 stav, Joshua Lochner, Hugo Larcher, Mathieu Morlon, Lewis Tunstall, Leandro Von Werra, and  
 609 Thomas Wolf. SmolVLM: Redefining small and efficient multimodal models. In *Second Con-  
 610 ference on Language Modeling*, 2025. URL <https://openreview.net/forum?id=qMUbhGUFB>.

613 Ahmed Masry, Do Xuan Long, Jia Qing Tan, Shafiq Joty, and Enamul Hoque. ChartQA: A bench-  
 614 mark for question answering about charts with visual and logical reasoning. In Smaranda Mure-  
 615 san, Preslav Nakov, and Aline Villavicencio (eds.), *Findings of the Association for Computational  
 616 Linguistics: ACL 2022*, pp. 2263–2279, Dublin, Ireland, May 2022. Association for Compu-  
 617 tational Linguistics. doi: 10.18653/v1/2022.findings-acl.177. URL <https://aclanthology.org/2022.findings-acl.177/>.

618 Minesh Mathew, Dimosthenis Karatzas, and CV Jawahar. Docvqa: A dataset for vqa on document  
 619 images. In *Proceedings of the IEEE/CVF winter conference on applications of computer vision*,  
 620 pp. 2200–2209, 2021.

622 Minesh Mathew, Viraj Bagal, Rubén Tito, Dimosthenis Karatzas, Ernest Valveny, and CV Jawahar.  
 623 Infographicvqa. In *Proceedings of the IEEE/CVF Winter Conference on Applications of Computer  
 624 Vision*, pp. 1697–1706, 2022.

626 Long Ouyang, Jeffrey Wu, Xu Jiang, Diogo Almeida, Carroll Wainwright, Pamela Mishkin, Chong  
 627 Zhang, Sandhini Agarwal, Katarina Slama, Alex Ray, et al. Training language models to fol-  
 628 low instructions with human feedback. *Advances in neural information processing systems*, 35:  
 629 27730–27744, 2022.

630 Alexander Michael Rombach and Peter Fettke. Deep learning based key information extraction from  
 631 business documents: Systematic literature review. *ACM Computing Surveys*, 2024.

633 Keshav Santhanam, Omar Khattab, Jon Saad-Falcon, Christopher Potts, and Matei Zaharia.  
 634 Colbertv2: Effective and efficient retrieval via lightweight late interaction. *arXiv preprint  
 635 arXiv:2112.01488*, 2021.

636 John Schulman, Philipp Moritz, Sergey Levine, Michael Jordan, and Pieter Abbeel. High-  
 637 dimensional continuous control using generalized advantage estimation. *arXiv preprint  
 638 arXiv:1506.02438*, 2015.

640 John Schulman, Filip Wolski, Prafulla Dhariwal, Alec Radford, and Oleg Klimov. Proximal policy  
 641 optimization algorithms. *arXiv preprint arXiv:1707.06347*, 2017.

642 Zhihong Shao, Peiyi Wang, Qihao Zhu, Runxin Xu, Junxiao Song, Xiao Bi, Haowei Zhang,  
 643 Mingchuan Zhang, YK Li, Y Wu, et al. Deepseekmath: Pushing the limits of mathematical  
 644 reasoning in open language models. *arXiv preprint arXiv:2402.03300*, 2024.

646 Huatong Song, Jinhao Jiang, Yingqian Min, Jie Chen, Zhipeng Chen, Wayne Xin Zhao, Lei Fang,  
 647 and Ji-Rong Wen. R1-searcher: Incentivizing the search capability in llms via reinforcement  
 learning. *arXiv preprint arXiv:2503.05592*, 2025.

648 Ryota Tanaka, Kyosuke Nishida, Kosuke Nishida, Taku Hasegawa, Itsumi Saito, and Kuniko Saito.  
 649 Slidevqa: a dataset for document visual question answering on multiple images. In *Proceedings*  
 650 *of the Thirty-Seventh AAAI Conference on Artificial Intelligence and Thirty-Fifth Conference on*  
 651 *Innovative Applications of Artificial Intelligence and Thirteenth Symposium on Educational Ad-*  
 652 *vances in Artificial Intelligence, AAAI'23/IAAI'23/EAAI'23*. AAAI Press, 2023a. ISBN 978-1-  
 653 57735-880-0. doi: 10.1609/aaai.v37i11.26598. URL <https://doi.org/10.1609/aaai.v37i11.26598>.

654

655 Ryota Tanaka, Kyosuke Nishida, Kosuke Nishida, Taku Hasegawa, Itsumi Saito, and Kuniko Saito.  
 656 Slidevqa: A dataset for document visual question answering on multiple images. In *Proceedings*  
 657 *of the AAAI Conference on Artificial Intelligence*, volume 37, pp. 13636–13645, 2023b.

658

659 Rubèn Tito, Dimosthenis Karatzas, and Ernest Valveny. Hierarchical multimodal transformers for  
 660 multipage docvqa. *Pattern Recogn.*, 144(C), December 2023a. ISSN 0031-3203. doi: 10.1016/j.  
 661 patcog.2023.109834. URL <https://doi.org/10.1016/j.patcog.2023.109834>.

662

663 Rubèn Tito, Dimosthenis Karatzas, and Ernest Valveny. Hierarchical multimodal transformers for  
 664 multipage docvqa. *Pattern Recognition*, 144:109834, 2023b.

665 Jordy Van Landeghem, Rubèn Tito, Łukasz Borchmann, Michał Pietruszka, Paweł Joziaik, Rafal  
 666 Powalski, Dawid Jurkiewicz, Mickaël Coustaty, Bertrand Anckaert, Ernest Valveny, et al. Docu-  
 667 ment understanding dataset and evaluation (dude). In *Proceedings of the IEEE/CVF International*  
 668 *Conference on Computer Vision*, pp. 19528–19540, 2023.

669

670 Kangrui Wang, Pingyue Zhang, Zihan Wang, Yaning Gao\*, Linjie Li, Qineng Wang, Hanyang Chen,  
 671 Chi Wan, Yiping Lu, Zhengyuan Yang, Lijuan Wang, Ranjay Krishna, Jiajun Wu, Li Fei-Fei, Yejin  
 672 Choi, and Manling Li. Reinforcing visual state reasoning for multi-turn vlm agents, 2025a. URL  
 673 <https://github.com/RAGEN-AI/VAGEN>.

674

675 Liang Wang, Nan Yang, Xiaolong Huang, Binxing Jiao, Linjun Yang, Dixin Jiang, Rangan Ma-  
 676 jumder, and Furu Wei. Text embeddings by weakly-supervised contrastive pre-training. *arXiv*  
 677 *preprint arXiv:2212.03533*, 2022.

678

679 Peng Wang, Shuai Bai, Sinan Tan, Shijie Wang, Zhihao Fan, Jinze Bai, Keqin Chen, Xuejing Liu,  
 680 Jialin Wang, Wenbin Ge, Yang Fan, Kai Dang, Mengfei Du, Xuancheng Ren, Rui Men, Dayiheng  
 681 Liu, Chang Zhou, Jingren Zhou, and Junyang Lin. Qwen2-vl: Enhancing vision-language model's  
 682 perception of the world at any resolution. *arXiv preprint arXiv:2409.12191*, 2024.

683

684 Quchen Wang, Ruixue Ding, Zehui Chen, Weiqi Wu, Shihang Wang, Pengjun Xie, and Feng Zhao.  
 685 Vidorag: Visual document retrieval-augmented generation via dynamic iterative reasoning agents.  
 686 *arXiv preprint arXiv:2502.18017*, 2025b.

687

688 Weiyun Wang, Zhangwei Gao, Lixin Gu, Hengjun Pu, Long Cui, Xingguang Wei, Zhaoyang Liu,  
 689 Linglin Jing, Shenglong Ye, Jie Shao, et al. Internvl3. 5: Advancing open-source multimodal  
 690 models in versatility, reasoning, and efficiency. *arXiv preprint arXiv:2508.18265*, 2025c.

691

692 Zilong Wang, Yichao Zhou, Wei Wei, Chen-Yu Lee, and Sandeep Tata. Vrd: A benchmark for  
 693 visually-rich document understanding. In *Proceedings of the 29th ACM SIGKDD Conference on*  
 694 *Knowledge Discovery and Data Mining*, pp. 5184–5193, 2023.

695

696 Xudong Xie, Hao Yan, Liang Yin, Yang Liu, Jing Ding, Minghui Liao, Yuliang Liu, Wei Chen, and  
 697 Xiang Bai. Wukong: A large multimodal model for efficient long pdf reading with end-to-end  
 698 sparse sampling. *arXiv preprint arXiv:2410.05970*, 2024.

699

700 Yifei Zhou, Andrea Zanette, Jiayi Pan, Sergey Levine, and Aviral Kumar. ArCHer: Training lan-  
 701 guage model agents via hierarchical multi-turn RL. In *Forty-first International Conference on*  
 702 *Machine Learning*, 2024. URL <https://openreview.net/forum?id=b6rA0kAHT1>.

703

704 Daniel M Ziegler, Nisan Stiennon, Jeffrey Wu, Tom B Brown, Alec Radford, Dario Amodei, Paul  
 705 Christiano, and Geoffrey Irving. Fine-tuning language models from human preferences. *arXiv*  
 706 *preprint arXiv:1909.08593*, 2019.

702 A DATASETS  
703704 A.1 TRAINING DATASET  
705706 **Training.** We construct our training dataset by combining samples from three publicly available  
707 multi-page document understanding datasets: DUDE (Van Landeghem et al., 2023), MP-  
708 DocVQA (Tito et al., 2023a), and SlideVQA Tanaka et al. (2023a). These datasets provide diverse  
709 document layouts and question-answering formats, making them well-suited for training models on  
710 complex multi-turn document question answering tasks.711 DUDE is a large-scale benchmark designed for multi-page, visually rich document understanding.  
712 It covers diverse domains such as scientific articles, financial and legal reports, technical manuals,  
713 and presentations. Each example consists of a full PDF document rendered into page images, paired  
714 with a natural-language query and a free-form textual answer, along with page-level ground-truth  
715 evidence annotations. SlideVQA contains questions grounded in slide decks, where understanding  
716 layout and inter-slide referencing is crucial. It contains slide decks from diverse topics such as  
717 education, business, and research talks, requiring models to reason across sequential pages that mix  
718 text, charts, and images. Each example provides a slide deck rendered as ordered page images,  
719 a natural-language question, and a free-form textual answer, with annotations of relevant slides for  
720 evidence grounding. MPDocVQA extends the traditional single-page VQA setting (originally based  
721 on DocVQA) by concatenating additional pages to the original single-page input, while retaining  
722 the same set of user questions. However, since many of these questions were authored under the  
723 assumption that only one page is visible (e.g., “What is the date?” or “Who is the author?”), they  
724 often lack sufficient context to guide document retrieval or navigation. To address this, we first use  
725 GPT-4o (Hurst et al., 2024) to automatically identify this kind of samples. Then we integrate the  
726 index of referred pages into the questions to get page-index-referenced questions, e.g., “In page 5,  
727 what is the date?”. The prompt we used is shown below:  
728729 **Prompt for Filtering Queries**730 You are given a question from a multi-page document VQA dataset. Some questions are not  
731 suitable for training an agent to autonomously locate the target page, because they assume  
732 the agent already knows which page is relevant. These questions are often vague, layout-  
733 based, or refer to elements only visible on a known page (e.g., “What is the PVR no given  
734 in the approval sheet?”, or “What is written at the top right?”). Your task is to assign a label  
735 to each question:736 - 1 if the question belongs to this kind of problem, i.e., it assumes the correct page is known  
737 and cannot be answered without it.  
738 - 0 if the question does not belong to this kind of problem, i.e., it can be answered after  
739 locating the page based on content in the question.

740 Respond with a JSON object containing only the field “label”. Examples:

741 Question: What is the PVR no given in the approval sheet? Answer: { “label”: 1 }  
742 Question: What is the project name mentioned in the title block? Answer: { “label”: 0 }  
743 Question: What is the symposium organized by Division of Agricultural and Food Chemistry? Answer: { “label”: 0 }  
744 Question: What is written on the top right corner? Answer: { “label”: 1 }  
745 Question: What is the page number? Answer: { “label”: 1 }  
746 Question: What is the Date? Answer: { “label”: 1 }  
747 Now, label the following question:

748 Question: {question}

749 To ensure that our model is consistently exposed to multi-page reasoning scenarios, we additionally  
750 discard any documents with fewer than 10 pages from all three datasets. This helps avoid biasing  
751 the model toward short-context behavior and ensures a consistent level of document complexity.  
752753 After merging and filtering, we obtain a training set consisting of 30,728 samples, each comprising  
754 a user query and its corresponding multi-page document context, answer and the index of evi-  
755 dence pages. Finally, we proportionally sample 1,024 samples from the validation set of these three  
756 datasets as our validation set.

756 A.2 BENCHMARKS  
757

758 We evaluate our method on a diverse set of benchmarks: MMLongBench (Ma et al., 2024b), Long-  
759 DocURL (Deng et al., 2024), PaperTab (Hui et al., 2024), PaperText (Hui et al., 2024), and Fe-  
760 taTab (Hui et al., 2024). These datasets span a wide range of scenarios, including both open-domain  
761 and closed-domain tasks, and include textual as well as visual content. The documents also vary in  
762 length and structure, ranging from short forms to complex, multi-page documents. This diversity en-  
763 sures a comprehensive and fair evaluation of our model’s performance across real-world document  
764 understanding tasks.

765 • **MMLongBench-Doc** is a large-scale benchmark designed to evaluate how multimodal large lan-  
766 guage models handle long, visually rich documents. It contains over a thousand expert-annotated  
767 questions drawn from lengthy PDFs (averaging 50 pages and 20k tokens) that mix text, tables,  
768 charts, and images. Tasks require single-page, cross-page, and sometimes unanswerable reason-  
769 ing, testing a model’s ability to retrieve and integrate evidence across multiple modalities and  
770 extended contexts.

771 • **LongDocURL** is a benchmark for evaluating large vision-language models on long, multimodal  
772 documents by combining three core task types: understanding, numerical reasoning, and element  
773 locating. It includes 2,325 high-quality question-answer pairs over 396 documents totaling over  
774 33,000 pages, with an average of 85.6 pages per document. Tasks vary in their evidence require-  
775 ments: some require single-page evidence, others multi-page, and many involve locating evidence  
776 across different layout elements (text, tables, figures, and layout).

777 • **PaperText** is a subset in the UDA benchmark made up of academic papers (in PDF form) used for  
778 retrieval-augmented generation / document question answering tasks. Each document comes with  
779 multiple question-answer pairs drawn from “Qasper” (an academic paper reading comprehension  
780 dataset), where questions may be extractive, yes/no, or free-form. The dataset preserves full  
781 documents to allow answering from context, rather than just small passages.

782 • **PaperTab** is another subset in UDA also based on academic papers, but the focus is on Q&A  
783 pairs where evidence comes from or interacts with tables inside papers. Like PaperText, it retains  
784 full PDF documents so that models must locate and reason over tabular content, as well as textual  
785 content. The questions are similarly diverse (extractive, yes/no, free-form), and the average size  
786 is modest ( 10–11 pages per document).

787 • **FetaTab** is a subset of the UDA (Unstructured Document Analysis) benchmark that focuses on  
788 free-form question answering over Wikipedia tables in both HTML and PDF formats. It comprises  
789 878 documents and 1,023 QA pairs, averaging about 14.9 pages per document. The questions are  
790 “free-form” (i.e. natural language answers, not limited to extractive spans or simple yes/no),  
791 which requires models to understand table content, context, and sometimes cross-format layout.

792 B BASELINES  
793

794 To evaluate the effectiveness of ALDEN, we compare it against three categories of methods:  
795

796 • **Base VLMs supporting multi-image input.** These models directly take the entire multi-page  
797 document as context without retrieval, leveraging their built-in multi-page visual processing ca-  
798 pabilities. For fairness, we select open-source VLMs of similar scale to Qwen2.5-VL-7B, in-  
799 cluding LLaVA-v1.6-Mistral-7B (Liu et al., 2024a), Phi-3.5-Vision-Instruct (Abdin et al., 2024),  
800 LLaVA-One-Vision-7B (Li et al., 2024), SmolVLM-Instruct (Marafioti et al., 2025), mPLUG-  
801 DocOwl2 (Hu et al., 2024), LEOPARD (Jia et al., 2024), InternVL3.5-8B-Instruct (Wang et al.,  
802 2025c).

803 • **Visual RAG methods.** These methods use the user query to retrieve the most relevant document  
804 pages and feed them into the model as context. We include M3DocRAG (Cho et al., 2024) as a  
805 strong baseline, as well as our proposed ALDEN. To isolate the impact of our reward function  
806 design, we additionally evaluate a variant that trains the same backbone with GRPO using only  
807 outcome-based rewards (no turn-level shaping), mirroring common text-only RLHF setups as in  
808 ReSearch (Chen et al., 2025b). Specifically,  
809 – M3DocRAG is a multi-modal document understanding framework designed for multi-page  
and multi-document question answering. It first encodes each page into joint visual-text em-

810 beddings using a multi-modal encoder, then retrieves the top-K relevant pages via a MaxSim-  
 811 based retrieval mechanism, optionally accelerated with FAISS for large-scale documents.  
 812 Finally, a multi-modal language model processes the retrieved pages to generate precise an-  
 813 swers, effectively handling complex queries that require reasoning over both textual and vi-  
 814 sual content.

815 – ReSearch introduces a framework that trains large language models to integrate reasoning  
 816 and search in a unified process. The model learns, via reinforcement learning, when and  
 817 how to perform search actions during multi-step reasoning, using search results to guide  
 818 subsequent reasoning steps. By treating search as part of the reasoning chain, ReSearch  
 819 enables LLMs to solve complex multi-hop tasks, demonstrate self-correction and reflection,  
 820 and generalize effectively across benchmarks, achieving significant performance gains over  
 821 baseline models.

822 • **Hybrid RAG methods.** These approaches combine visual and textual retrieval by first applying  
 823 an OCR tool to extract all text from the document. The query is then used to retrieve both the  
 824 most relevant page image and the most relevant OCR-extracted text, which are jointly fed into  
 825 the model. We evaluate MDocAgent (Han et al., 2025) and VidoRAG (Wang et al., 2025b) as a  
 826 representative method in this category.

827 – MDocAgent is a multi-modal, multi-agent framework for document understanding that com-  
 828 bines Retrieval-Augmented Generation (RAG) with specialized agents to handle complex  
 829 documents. The system employs a General Agent for multi-modal context retrieval, a Crit-  
 830 ical Agent for identifying key information, a Text Agent for analyzing textual content, an  
 831 Image Agent for interpreting visual elements, and a Summarizing Agent to synthesize re-  
 832 sults. By coordinating these agents, MDocAgent effectively integrates textual and visual  
 833 reasoning, achieving significant improvements in accuracy and error reduction compared to  
 834 existing large vision-language models and RAG-based methods. For all five agents in this  
 835 framework, we consistently use the original LLaMA3.1-8B as the LLM for the text agent,  
 836 while employing a consistent VLMs, i.e., Qwen2.5-VL-7B, for remaining agents.

837 – ViDoRAG is a multi-agent framework designed to enhance the understanding of visually rich  
 838 documents. It employs a Gaussian Mixture Model (GMM)-based hybrid retrieval strategy  
 839 to effectively handle multi-modal retrieval, integrating both textual and visual information.  
 840 The framework incorporates a dynamic iterative reasoning process, utilizing agents such as  
 841 Seeker, Inspector, and Answer to iteratively refine the understanding and generation of re-  
 842 sponses. This approach addresses challenges in traditional Retrieval-Augmented Generation  
 843 (RAG) methods by improving retrieval accuracy and enabling complex reasoning over visual  
 844 documents. We use Qwen2.5-VL-7B as backbone for all agents in this methods.

## 845 C IMPLEMENTATION DETAILS

846 Our implementation is based on the EasyR1<sup>1</sup> framework. Both the policy model and the value  
 847 function are initialized from Qwen2.5-VL-7B-Instruct (Bai et al., 2025). We use a batch size of 128,  
 848 with fixed learning rates of  $1 \times 10^{-6}$  for the policy model and  $1 \times 10^{-5}$  for the value function.  
 849 The maximum number of interaction turns is set to  $T = 6$ . For visual inputs, we constrain the  
 850 number of image pixels to lie between 261,070 and 2,508,800. Based on these settings, we set the  
 851 maximum number of tokens in the trajectory as 19000. The KL coefficients for generated tokens  
 852 and observation tokens are set to  $\beta_{\text{gen}} = 0.001$  and  $\beta_{\text{obs}} = 0.01$ , respectively. For the search  
 853 actions, we used only the top-1 retrieved pages. While calculating the  $NDCG@m$  metrics, we set  
 854  $m$  as 5 to avoid sparse, all zero rewards. Besides, we set the scale coefficient  $\alpha = 5$ . The weight  
 855 of repetition penalty is set as  $\eta = 0.5$ . For the calculation of GAE, we set  $\gamma_{\text{token}} = 1.0$ ,  $\gamma_{\text{turn}} = 0.9$   
 856 and  $\lambda_{\text{token}} = \lambda_{\text{turn}} = 1.0$ . During training, we adopt the single-vector retriever vdr-2b-v1 (Ma et al.,  
 857 2024a) for images and e5-large-v2 (Wang et al., 2022) for text for training efficiency. For evaluation,  
 858 we also report results with the multi-vector retrievers ColQwen2-v1.0 (ColQwen) (Faysse et al.,  
 859 2025) for images and ColBERT-v2.0 (ColBERT) (Santhanam et al., 2021) for text. All experiments  
 860 are conducted on 16 NVIDIA A100-80Gb GPUs.

861 The system prompt that we used during training of Visual RAG variant of ALDEN is shown here:

862  
 863 <sup>1</sup><https://github.com/hiyoga/EasyR1>

864  
865**System prompt of ALDEN with Visual RAG**866  
867  
868  
869  
870  
871  
872  
873  
874  
875  
876  
877  
878  
879  
880

You are a helpful assistant designed to answer user questions based on a user-provided multi-page document. The document can not be input directly with the question, you must reason step by step to determine how to obtain evidence document pages by optimally utilizing tools and analyze the relevant content in the obtained document pages to precisely answer user's question. Your reasoning process MUST BE enclosed within `<think> </think>` tags. Your answer MUST BE enclosed within `<answer> </answer>` tags. In the last part of the answer, the final exact answer is enclosed within `\boxed{\{\}}` with latex format. The available tool is a \*\*search tool\*\*. After reasoning, you can invoke the search tool by generating `<search> your search query here </search>` to retrieve document pages most relevant to your search query. For example, your response could be in the format of '`<think> your reasoning process </think> <search> search query </search>`', or '`<think> your reasoning process </think> <answer> your answer here`'. The final answer is `\[ \boxed{\{answer here\}} \] </answer>`'. After invoking a tool, the user will return obtained document pages inside `<result> </result>` tags to you. Besides, the user will additionally provide the page number of the obtained page.

\*\*Important constraints\*\*:

- Only if you get all the potential evidence pages and find that the there is no evidenced answer or the document content is irrelevant to the user query, you can respond with '`<think> your reasoning process </think> <answer> The final answer is \[ \boxed{The problem is not answerable} \] </answer>`'.
- If multiple valid answers are found, return them separated by semicolons.
- You may not get the true evidence page in one-shot, carefully check whether the obtained pages are the true evidence page. If not, try different rewritings of your query or try different tool usage strategy several times.

888  
889  
890  
891  
892  
893  
894  
895  
896  
897  
898  
899  
900  
901  
902  
903  
904  
905  
906  
907  
908  
909  
910  
911  
912  
913  
914  
915  
916  
917

The system prompt that we used during training of Hybrid RAG variant of ALDEN is shown here

918  
919**System prompt of ALDEN with Hybrid RAG**920  
921  
922  
923  
924  
925  
926  
927  
928  
929  
930  
931  
932  
933  
934  
935  
936  
937  
938  
939  
940  
941

You are a helpful assistant designed to answer user questions based on a user-provided multi-page document. Each page exists in two modalities: the original image and an OCR text extraction. You cannot access the full document directly; instead, you must reason step by step to determine how to obtain evidence document pages by optimally utilizing tools and analyze the relevant content in the obtained document pages to precisely answer user's question. Your reasoning process **MUST BE** enclosed within `<think> </think>` tags. Your answer **MUST BE** enclosed within `<answer> </answer>` tags. In the last part of the answer, the final exact answer should be enclosed within `\boxed{\{\}}` with latex format. The available tools include a **\*\*search tool\*\*** and a **\*\*fetch tool\*\***. After reasoning, you can invoke either the search tool by generating `<search>` your search query here `</search>` to retrieve relevant document pages in both modalities or the fetch tool by generating `<fetch>` modal, page number `</fetch>` to obtain a specific document page in the specified modal, where the modal should be 'image' or 'text' and the page number should be a integrity number chosen from the user specified page number range. For example, your response could be in the format of '`<think>` your reasoning process `</think> <search>` search query `</search>`', or '`<think>` your reasoning process `</think> <fetch>` image, page number `</fetch>`', or '`<think>` your reasoning process `</think> <fetch>` text, page number `</fetch>`', or '`<think>` your reasoning process `</think> <answer>` your answer here. The final answer is `\[ \boxed{\{\text{answer here}\}} \] </answer>`'. After invoking a tool, the user will return obtained document pages inside `<result> </result>` tags to you. For the search tool, the user will return both the relevant image pages and the relevant OCR text pages and attach them with corresponding page numbers. For the fetch tool, the user will only return either the image page or the OCR text page according to your input arguments.

**\*\*Important constraints\*\*:**

- Only if you get all the potential evidence pages and find that the there is no evidenced answer or the document content is irrelevant to the user query, you can respond with '`<think>` your reasoning process `</think> <answer>` The final answer is `\[ \boxed{\{\text{The problem is not answerable}\}} \] </answer>`'.
- If multiple valid answers are found, return them separated by semicolons.
- Only one page can be fetched at a time using the fetch tool.
- You may not get the true evidence page in one-shot, carefully check whether the obtained pages are the true evidence page. If not, try different rewritings of your query or try different tool usage strategy several times.
- Page numbers shown in the document pages may not be consistent with user specified page number range. In case of any discrepancy, the user defined parge number range shall prevail.
- You need to invoke the tools at least once and can invoke up to 5 times. When you output the answer, the interaction stops.

954

955

**D EVALUATION METRICS**

956

We evaluate models using both answer quality and intermediate navigation metrics.

957

**Model-based Accuracy (Acc).** Answer quality is assessed with an LLM-as-judge protocol. Given a predicted answer and the ground-truth reference, GPT-4o is prompted to classify the prediction as *Correct*, *Incorrect*, or *Tie/Unclear*. We compute accuracy for each benchmark as the percentage of responses judged *Correct* over all responses:

958  
959  
960  
961  
962  
963

$$\text{Acc} = \frac{\#\text{Correct}}{N}, \quad (10)$$

where  $N$  is the number of test instances.

964

**Trajectory-level Recall (Rec).** Let  $\mathcal{G}$  denote the set of ground-truth evidence pages for a given query, and let  $\mathcal{T}$  denote the set of pages collected by the agent along a trajectory. The trajectory-level recall is defined as:

965  
966  
967  
968  
969  
970  
971

$$\text{Rec} = \frac{|\mathcal{T} \cap \mathcal{G}|}{|\mathcal{G}|}. \quad (11)$$

---

972  
 973  
 974  
 975  
 976  
 977  
 978  
 979  
 980  
 981  
 982  
 983  
 984  
 985 **Algorithm 1** PPO with Dual KL Regularization for Multi-Turn VRDU Agents  
 986  
 987 **Require:** Actor  $\pi_\theta$ , Critic  $V_\phi$ , Reference model  $\pi_{\text{ref}}$ , KL weights  $\beta_{\text{gen}}, \beta_{\text{obs}}$ , discount factors  
 $\gamma_{\text{token}}, \gamma_{\text{turn}}$ , GAE parameters  $\lambda_{\text{token}}, \lambda_{\text{turn}}$ , replay buffer  $\mathcal{B}$   
 988 1: Initialize replay buffer  $\mathcal{B}$   
 989 2: **for** iteration = 1, 2, . . . **do**  
 990 3:   Sample  $|\mathcal{B}|$  queries from the dataset  
 991 4:   **for** each query **do**  
 992 5:     Reset: query  $q$ , empty retrieval history,  $t \leftarrow 1$   
 993 6:     **while**  $t < T$  **and**  $a_{t-1} \neq \text{answer}$  **do**  
 994 7:        $\pi_\theta$  generates a token sequence  $a_t \sim \pi_\theta(\cdot|s_t)$   
 995 8:       Parse the discrete action (search, fetch, or answer) from  $a_t$   
 996 9:       Execute action  $\rightarrow$  obtain new state  $s_{t+1}$  and turn reward  $r_t$   
 997 10:      Store  $\{a_t, s_{t+1}, r_t\}$  in  $\mathcal{B}$   
 998 11:       $t \leftarrow t + 1$   
 999 12:     **Turn-level value estimation:**  
 1000 13:     **for** each episode in  $\mathcal{B}$  **do**  
 1001 14:       Estimate  $V_\phi(s_t)$  at final token of each turn  
 1002 15:       Compute target turn value  $\hat{V}_t$  via turn-level GAE  
 1003 16:       Assign token-level reward  $\tilde{r}_t \leftarrow \hat{V}_t$   
 1004 17:     **Dual KL penalty computation:**  
 1005 18:     **for** each token in  $\mathcal{B}$  **do**  
 1006 19:       **if** token is generated **then**  
 1007 20:         Compute  $A_t^i$  via token-level GAE using  $\tilde{r}_t$   
 1008 21:         Compute  $\text{KL}(\pi_\theta(\cdot|s) \parallel \pi_{\text{ref}}(\cdot|s))$  with weight  $\beta_{\text{gen}}$   
 1009 22:       **else if** token is observation **then**  
 1010 23:         Compute  $\text{KL}(\pi_\theta(\cdot|s) \parallel \pi_{\text{ref}}(\cdot|s))$  with weight  $\beta_{\text{obs}}$   
 1011 24:     **PPO update:**  
 1012 25:     Update  $\theta$  by maximizing policy loss  $\mathcal{L}_{\text{policy}}$   
 1013 26:     Update  $\phi$  by minimizing value loss  $\mathcal{L}_{\text{value}}$   
 1014  
 1015  
 1016  
 1017  
 1018  
 1019  
 1020  
 1021  
 1022  
 1023  
 1024  
 1025

---

1026 This metric measures the fraction of ground-truth pages successfully retrieved by the agent over the  
 1027 course of a trajectory, providing an indicator of how effectively the agent gathers relevant information.  
 1028

1029 **Trajectory-level Precision (Pre).** Let  $\mathcal{G}$  denote the set of ground-truth evidence pages for a given  
 1030 query, and let  $\mathcal{T}$  denote the set of pages collected by the agent along a trajectory. The trajectory-level  
 1031 precision is defined as:  
 1032

$$1033 \text{Pre} = \frac{|\mathcal{T} \cap \mathcal{G}|}{|\mathcal{T}|}. \quad (12)$$

$$1034$$

$$1035$$

1036 This metric measures the fraction of pages collected by the agent that are actually relevant, providing  
 1037 an indicator of how accurately the agent identifies evidence pages during a trajectory.  
 1038

1039 **F1 Score (F1).** Based on the trajectory-level precision and recall, the trajectory-level F1 score is  
 1040 defined as the harmonic mean of the two:  
 1041

$$1042 \text{F1} = 2 \cdot \frac{\text{Pre} \cdot \text{Rec}}{\text{Prec} + \text{Rec}}. \quad (13)$$

$$1043$$

1044 This metric provides a balanced measure of the agent’s performance, accounting for both its ability  
 1045 to collect relevant pages (recall) and to avoid collecting irrelevant ones (precision) over a trajectory.  
 1046

1047 **Number of uniquely collected pages (#UP).**

## 1049 E CASE STUDY

1050 In this section, we present typical examples from the LongDocURL benchmark to analyze the be-  
 1051 havior of the ALDEN model. As illustrated in the successful cases in Tab. 6 and Tab. 7, the agent  
 1052 effectively learns to combine the `search` and `fetch` actions to gather evidence and correctly an-  
 1053 swer the question. In particular, the example in Tab. 7 shows the agent using `fetch` to complement  
 1054 `search` when the latter fails to retrieve the true evidence page in a single step, highlighting the  
 1055 benefit of ALDEN’s expanded action space. Alongside these successes, we also present failure  
 1056 cases in Tab. 8 and Tab. 9. These examples reveal that the model still struggles to verify evidence  
 1057 pages and explore sufficiently when the `search` action returns results far from the ground-truth  
 1058 pages—a challenge we leave for future work.  
 1059

1060

1061

1062

1063

1064

1065

1066

1067

1068

1069

1070

1071

1072

1073

1074

1075

1076

1077

1078

1079

---

1080	
1081	
1082	
1083	
1084	
1085	
1086	
1087	
1088	
1089	
1090	<b>User Question</b>
1091	What's name of the figure at the page which contains a table whose name is "Table 18: Quality control related uses by type of use"?
1092	<b>Ground-truth</b>
1093	40
1094	<b>Pages</b>
1095	<b>Generated Tra-</b>
1096	<b>jectory</b>
1097	<b>assistant</b>
1098	<think> The question asks for the name of the figure at the page that con-
1099	tains a table with the name "Table 18: Quality control related uses by type
1100	of use". To answer this, I should use the search tool to look for the table
1101	with the specified name in the document. The fetch tool can be used to ob-
1102	tain the specific page where this table is located. </think> <search>
1103	name of the figure at the page which contains a table whose name is "Table
1104	18: Quality control related uses by type of use" </search>
1105	<b>user</b>
1106	<result> Page 39: Image tokens </result>
1107	<b>assistant</b>
1108	<think> The table mentioned in the search query is not found on the
1109	provided page. The table in the document is "Table 17: Regulatory uses
1110	by main types of uses". The search query asks for the figure at the page
1111	which contains the table "Table 18: Quality control related uses by type of
1112	use". I should use the fetch tool to obtain the page with the table "Table
1113	18: Quality control related uses by type of use". </think> <fetch> 40
1114	</fetch>
1115	<b>user</b>
1116	<result> Image tokens </result>
1117	<b>assistant</b>
1118	<think> The table mentioned in the search query is found on the pro-
1119	vided page. The table in the document is "Table 18: Quality control related
1120	uses by type of use". The search query asks for the figure at the page
1121	which contains the table "Table 18: Quality control related uses by type of
1122	use". The figure mentioned in the document is "Figure 20: Evolution of
1123	total numbers of uses of animals for pyrogenicity testing between 2015 and
1124	2018". The figure name is "Figure 20". </think> <answer> The final
1125	answer is \[ \box{Figure 20} \] </answer>

---

Table 6: Example of a generated case showing the user question and ALDEN's full reasoning–action trajectory.

1125  
1126  
1127  
1128  
1129  
1130  
1131  
1132  
1133

User Question	What is the percentage decrease in hospitalizations between May 14 and May 20, 2020? (A). -6.5(B). +6.5(C). -65(D). +65Choose the letter name in front of the right option from A, B, C, D.
Ground-truth Pages	21
Generated Trajectory	<p><b>assistant</b>  &lt;think&gt; The question asks for the percentage decrease in hospitalizations between May 14 and May 20, 2020. To answer this, I need to find information in the document that discusses hospitalizations for these specific dates and the percentage change between them. I will use the search tool to look for the relevant information in the document. &lt;/think&gt; &lt;search&gt; percentage decrease in hospitalizations between May 14 and May 20, 2020 &lt;/search&gt;</p> <p><b>user</b></p> <p>&lt;result&gt;Page 21: Image tokens &lt;/result&gt;</p> <p><b>assistant</b></p> <p>&lt;think&gt; The image contains the information needed to answer the question. According to the document, there has been a -6.5% decrease in hospitalized patients between May 14 and May 20, 2020. The correct answer is (A). &lt;/think&gt; &lt;answer&gt; The final answer is \[ \boxed{\{A\}} \]&lt;/answer&gt;</p>

Table 7: Example of a generated case showing the user question and ALDEN’s full reasoning–action trajectory.

User Question	What is the interval between specific lunar/solar events in days?
Ground-truth Pages	46, 47, 48, 55, 57, 58
Generated Trajectory	<p><b>assistant</b></p> <p>&lt;think&gt; The question asks for the interval between specific lunar/solar events in days. To answer this, I should look for information in the document that discusses lunar and solar events and their intervals. The search tool seems the best option to find this information. I will use the search tool first. &lt;/think&gt; &lt;search&gt; interval between lunar/solar events in days &lt;/search&gt;</p> <p><b>user</b></p> <p>&lt;result&gt;Page 25: Image tokens &lt;/result&gt;</p> <p><b>assistant</b></p> <p>&lt;think&gt; The image contains the information needed to answer the question. The document states that the interval between the lunar eclipse on April 15, 2014, and the lunar eclipse on September 28, 2015, is exactly 266 days. This matches the information in the question. The interval between specific lunar/solar events in days is 266 days. The final answer is \boxed{266} &lt;/think&gt; &lt;answer&gt; The final answer is \boxed{266} &lt;/answer&gt;</p>

Table 8: Example of a generated case showing the user question and ALDEN’s full reasoning–action trajectory.

1188

1189

1190

1191

1192

1193

1194

1195

1196

1197

1198

1199

1200

1201

1202

1203	<b>User Question</b>	What penalties are specified for possession of category 1 or category 2 items?
------	----------------------	--

1204	<b>Ground-truth Pages</b>	21
------	---------------------------	----

1205	<b>Generated Trajectory</b>	<b>assistant</b> <think> The question asks for the penalties specified for possession of category 1 or category 2 items. To answer this, I should look for information in the document that discusses the penalties for these categories. The search tool seems the best option to start with as it can help locate the relevant information in the document. I will use the search tool first. </think> <search> penalties for possession of category 1 or category 2 items </search> <b>user</b> <result>Page 21: Image tokens </result> <b>assistant</b> <think> The image contains the information needed to answer the question. According to the document, the penalties for possession of a category 1 item or a category 2 item are specified in the Misuse of Drugs Act 1981. For a simple offence, the penalty is \$12,000 or imprisonment for 3 years or both. The relevant information is found in the document. The final answer is \[ \boxed{\{\$12,000 or imprisonment for 3 years or both\}} \]</think> <answer> The final answer is \[ \boxed{\{\$12,000 or imprisonment for 3 years or both\}} \]</answer>
------	-----------------------------	--

Table 9: Example of a generated case showing the user question and ALDEN’s full reasoning–action trajectory.

1228

1229

1230

1231

1232

1233

1234

1235

1236

1237

1238

1239

1240

1241